Early stage inflammation changes in supraspinatus muscle after rotator cuff tear

Stengaard, Kira; Hejbøl, Eva Kildall; Jensen, Peter Toft; Degn, Matilda; Linh Ta, Thi My; Stensballe, Allan; Andersen, Ditte Caroline; Schrøder, Henrik Daa; Lambertsen, Kate Lykke; Frich, Lars Henrik

Published in:
Journal of Shoulder and Elbow Surgery

DOI (link to publication from Publisher):
10.1016/j.jse.2021.12.046

Publication date:
2022

Document Version
Publisher's PDF, also known as Version of record

J Shoulder Elbow Surg (2022) 31, 1344–1356

Journal of Shoulder and Elbow Surgery

www.elsevier.com/locate/ymse

Early-stage inflammation changes in supraspinatus muscle after rotator cuff tear

Kira Stengaard, MSc[a,1], Eva Kildall Hejbøl, PhD[b,1], Peter Toft Jensen, MSc[a], Matilda Degn, PhD[c], Thi My Linh Ta, MSc[a], Allan Stensballe, PhD[d], Ditte Caroline Andersen, PhD[e], Henrik Daa Schrøder, DMSc[f], Kate Lykke Lambertsen, PhD[a,g,h], Lars Henrik Frich, MD, PhD[a,b,i,*]

[a]*Department of Neurobiology Research, Institute of Molecular Medicine, University of Southern Denmark, Odense, Denmark*
[b]*Department of Orthopedics, Hospital Sønderjylland, Region of Southern Denmark, Denmark*
[c]*Pediatric Oncology Laboratory, Department of Pediatrics and Adolescent Medicine, University Hospital Rigshospitalet, Copenhagen, Denmark*
[d]*Department of Health Science and Technology, Aalborg University, Aalborg, Denmark*
[e]*Department of Clinical Biochemistry and Pharmacology, Odense University Hospital, Institute of Clinical Research, University of Southern, Denmark*
[f]*Department of Pathology, Odense University Hospital, Odense, Denmark*
[g]*Department of Neurology, Odense University Hospital, Odense, Denmark*
[h]*BRIDGE–Brain Research–Inter-Disciplinary Guided Excellence, Department of Clinical Research, University of Southern Denmark, Odense, Denmark*
[i]*Orthopedic Research Unit, Department of Regional Health Research, University of Southern Denmark, Odense, Denmark*

Background: Rotator cuff (RC) tendon tear leads to impaired shoulder function and pain. The supraspinatus (SS) tendon is most often affected, but the biological response of the SS muscle to SS tendon tear is largely unknown. This study aimed to investigate time-dependent muscle inflammation, degeneration, fatty infiltration, and regeneration in experimental SS tear conditions.
Methods: Forty-five C57BL/6 mice were subjected to SS tendon tear and allowed to recover for 1, 3, 5, 7, 14, or 28 days. The extent of muscle damage was examined using histologic, flow cytometric, proteomic, and chemiluminescence analyses.
Results: We found that muscle inflammation peaked around day 5 with increased monocyte infiltration and increased cytokine levels in the ipsilateral compared to the contralateral SS muscle. Bioinformatics analysis of proteomics on mice that survived 5 days after RC tendon tear revealed upregulated proteins involved in ''neutrophil activation involved in immune response'' and ''extracellular matrix organization,'' whereas ''skeletal muscle tissue development and contraction'' and ''respiratory electron transport chain'' were among the most downregulated. Histologic analysis of collagen showed increased collagen accumulation and fatty infiltration of the ipsilateral SS over time. Finally, we observed time- and lesion-dependent changes in satellite cell and fibro-adipogenic progenitor populations.
Conclusion: Altogether, we demonstrate that the SS muscle shows severe signs of acute inflammation, early degeneration, and fatty infiltration, as well as reduced regenerative potential following SS tendon tear.

This study was approved by the Danish Animal Inspectorate under the Danish Veterinary and Food Administration (Ref. no. 2013-15-2934-00924).

[1] These authors contributed equally to this work.

*Reprint requests: Lars Henrik Frich, MD, PhD, Department of Regional Health Research, University of Southern Denmark, J.B. Winsløwsvej 19, 5000 Odense C, Denmark 20274119.
E-mail address: lars.henrik.frich@rsyd.dk (L.H. Frich).

https://doi.org/10.1016/j.jse.2021.12.046

Level of evidence: Basic Science Study; Histology; Animal Model

Keywords: Rotator cuff tear; inflammation; skeletal muscle; proteomics; fatty infiltration; fibro-adipogenic progenitors

The prevalence of rotator cuff (RC) tears is high and increases markedly after 50 years of age[42] because of a combination of degeneration of the RC and trauma to the shoulder.[4,15] Supraspinatus (SS) tendon is most often involved, either solely or in combination with tears of 1 or more tendons.[8] Surgically repaired RC tendons tend to heal poorly as tear size increases[18,30] and degenerative changes in both tendons and muscles[20,21] enhance this effect.

Healthy skeletal muscle tissue contains very few adipocytes.[9] Fatty infiltration with adipocyte accumulation is linked to impaired RC muscle function in both humans and animals.[20,21,39] When atrophy prevails, the change in muscle volume is believed to be slightly reversible, whereas fatty infiltration in most cases seems to progress even though surgical repair of the RC is successful.[19,40] The biological changes in the RC muscles during tear conditions and healing after surgery are, however, far from fully understood.[45]

Recent data in humans and rodents have argued that the RC muscles become inflamed in the presence of RC tear,[16,17,23,33,37] and results from experimental RC tear models suggest that acute inflammation plays a detrimental role in the onset of chronic muscle damage following RC tears.[1,22,26] Inflammation is also known to influence the extent and subcellular changes leading to fatty infiltration in skeletal muscle.[24,36]

Muscle recovery depends on quiescent muscle stem cells, satellite cells, which normally are rapidly activated following increased muscle use or injury.[2] Satellite cells migrate, proliferate, and subsequently become integrated in myofibers. The efficiency of this process determines the success of muscle recovery. Although many aspects of how the initial inflammatory response supports early myogenesis are known, many details on the interaction remain unresolved. This is further complicated by the findings that satellite cells from RC muscles have reduced myogenic and increased adipogenic differentiation potential compared to muscles like the gastronemius,[34] suggesting that there may be both a cellular and epigenetic basis behind the poor rates of RC muscle healing.

We used a validated model of experimental SS tendon tear in C57BL/6 mice to study the inflammatory, degenerative, and regenerative responses of the SS muscle during the first 28 days after tendon tear.

Materials and methods

Mice

Forty-five adult C57BL/6 mice were purchased from Taconic Ltd. (Ry, Denmark) and transferred to the Laboratory of Biomedicine, University of Southern Denmark, where they were allowed to acclimatize for 2 weeks before surgery. Animals were housed under diurnal lighting conditions and given free access to food and water. All mice used in the present study were adult (12-16-week) males. All efforts were made to minimize pain and distress.

SS tendon tear mouse model

To mimic an acute SS tendon tear, we used a modified surgical procedure of that described by Bell et al.[5] Mice were anesthetized using a ketamine (100 mg/kg, VEDCO Inc.)–xylazine (10 mg/kg, VEDCO Inc.) cocktail injected intraperitoneally and positioned in a left lateral decubitus position on a heating pad under a surgical microscope. An incision was placed just above the elbow and directed posteriorly and superiorly toward the ear. The deltoid was identified and released from the acromion with sharp dissecting scissors. The proximal humerus was grasped for stability and externally rotated to visualize the coracoacromial arch. To visualize the SS tendon, blunt dissection was used between the humeral head and the coracoacromial arch. The SS tendon was sharply released using scissors, allowing the SS muscle to retract. The deltoid was reflected and the skin incision closed using no. 7-0 sutures. Mice were then injected with saline to prevent dehydration and given buprenorphine hydrochloride (0.001 mg/20 g body weight; Temgesic) 3 times at 8-hour intervals for postsurgical analgesia. Mice were housed separately in a recovery room and monitored for a 24-48-hour recovery period. Thereafter, mice were returned to the conventional animal facility.

Grip strength analysis

To evaluate surgical success after SS tendon tear, the grip strength meter (BIO-GT-3; BIOSEB, Vitrolles, France) was used to study muscular function. This test has previously been used successfully to monitor shoulder function in mice.[35] Peak amount of force was recorded in 5 sequential trials, and the highest grip value was recorded as the score.[12] We analyzed the grip strength in individual (left and right) front paws prior to (baseline) and 5 days after SS tendon tear. The unit of force measured is presented as grams.

Tissue processing

Mice used for histology were euthanized at days 1, 3, 5, 7, 14, and 28 (n = 2-3 mice/time point) using an overdose of pentobarbital (200 mg/mL) containing lidocaine (20 mg/mL) (Glostrup Apotek; Glostrup, Denmark) and perfused through the left ventricle with ice-cold 4% paraformaldehyde. Ipsilateral and nonlesioned contralateral SS muscles were dissected free and frozen with OCT compound (Tissue Tek, Sigma-Aldrich, Søborg, Denmark) and stored at –20°C until further processing. SS muscles were longitudinally cut into 6 parallel series of 16-µm-thick sections on a cryostat (LEICA CM3050S; Leica, Boston Industries, Inc., USA) and placed on gelatine-coated glass slides. Sections were stored at –20°C.

Mice used for flow cytometry were euthanized at days 5, 7, 14, and 28 (n = 4-5 mice/time point) using an overdose of pentobarbital (200 mg/mL) containing lidocaine (20 mg/mL) and perfused through the left ventricle using ice-cold phosphate-buffered saline (pH 7.4, Sigma-Aldrich, St. Louis, Missouri, USA); SS muscles were dissected and placed in Hanks buffered saline solution (Thermo Fischer Scientific, Odense, Denmark).

Mice (n = 8) used for proteomics and multiplex ELISA were killed on day 5 by cervical dislocation. The SS muscles were dissected and cut into halves in the frontal plane, one for multiplex analysis and one for proteomics. Biopsies were then frozen with dry ice and stored at −80°C until further processing.

Histology

Grading of collagen

Sections were stained with Sirius Red. Structural collagen changes were scored according to the following system: 0 = normal collagen content; 1 = collagen in the tendon inside the muscle was unstructured; 2 = collagen in the extracellular matrix (ECM) increased between the muscle fibers near the musculotendinous junction; 3 = collagen in the ECM increased between the fibers more peripherally in the muscle. The mean score of 11-13 sections from each muscle was calculated, n = 2-3 mice/time point.

Quantification of adipocytes

Sections were stained with Oil Red O (Sigma Aldrich). Only cells with a clear cell membrane and a red cytoplasm were counted. In addition, adipocytes were identified and counted in parallel hematoxylin-eosin– and Sirius Red–stained sections. The number of adipocytes was counted on 11-13 sections from each muscle (n = 2-3 mice/time point), and the mean number of adipocytes was calculated from the results from the 3 stains.

Flow cytometry

Isolation of cells

Each muscle was processed individually. Muscle dissociation was performed with the ''skeletal muscle dissociation kit'' (Miltenyi, Miltenyi Biotec, inc USA) using a gentleMACS octo dissociator according to the manufacturer's instructions. Next, tubes containing muscle homogenates were processed for flow cytometry as previously described.[28] Total number of living cells per milliliter was counted using a NucleoCounter (NC-200). Cells were stained for live/dead status using a Fixable Viability Dye eFluoro 506 (eBioscience, Thermo Scientific, Odense Denmark) and fixed using Cytofix/Cytoperm (BD Biosciences).

Flow cytometric analysis

Flow cytometry was performed as previously described[43] using BD LSR II (BD Biosciences) and FACSDiva 6.0 software (BD Biosciences). Cells were blocked with Syrian hamster immunoglobulin (50 µg/mL; Trichem, Skanderborg, Denmark) and Mouse BD FcBlock (1 µg/mL, BD Biosciences) diluted in FACS buffer to prevent nonspecific staining.

Cells were collected using forward scatter (FSC) and side scatter (SSC), followed by FSC area (FSC-A) / FSC height (FSC-H). Only living cells were included. Infiltrating blood-borne cells were identified as $CD45^+$ cells, leukocytes as $CD45^+CD11b^+$, T cells as $CD3^+CD45^+$, neutrophils as $CD45^+CD11b^+Ly6C^+Ly6G^+$, and macrophages as $CD45^+CD11b^+Ly6C^+Ly6G^-$. Satellite cells were identified as $CD45^-CD31^-Sca1^-\alpha7integrin^+$ cells. A subpopulation of $CD45^-$ cells consisting of fibro-adipogenic progenitors (FAPs) and endothelial cells were identified by Sca1 positivity. Positive staining was determined based on the fluorescence levels of the respective isotype and fluorescence minus one (FMO) controls. Antibodies were directly conjugated with fluorochromes: APC anti-CD3 (clone 145-2C11), PerCP Cy5.5 anti-CD45 (clone 30-F11), PE anti-CD11b (clone M1/70), PE Cy7 anti-Ly6C (clone AL-21), PE Cy7 anti-CD31 (all from BD Pharmingen, San Diego, CA, United States), PE anti-integrin α7 (Miltenyi), FITC anti-Ly6A/E (Sca1) (clone D7), and BV421 anti-Ly6G (clone 1A8) from BD Biosciences. Isotype controls used were hamster IgG1κ (clone A19-3), rat IgG2b (clone A95-1), mouse IgG1 (Miltenyi), rat IgMκ (clone R4-22), and rIgG2a (clone R35-95). The mean fluorescence intensity was calculated as the geometric mean of each population in the CD45- and CD11b-positive gates, respectively.

Multiplex analysis

Protein purification

Samples were prepared as previously described[28] and protein concentrations estimated using the Thermo Scientific Micro BCA Protein assay Kit (Pierce Chemical Co., Pierce Chemical 4722 Bronze Way Dallas, Texas).[28]

Multiplex analysis

Ipsilateral and nonlesioned contralateral SS muscle samples (n = 8/group) were analyzed on the MSD QuickPlex (SQ120) Plate Reader (Mesoscale, Rockville, Maryland) using a Mouse Proinflammatory V-Plex Plus Kit (IFNγ, IL-1β, IL-2, IL-4, IL-5, IL-6, IL-10, IL-12p70, CXCL1, TNF, Mesoscale) according to the manufacturer's instructions. Samples were run in duplex and diluted 2- or 4-fold in diluent 41 prior to measurement. Data were analyzed using MSD Discovery Workbench software. The lower limit of detection was a calculated concentration based on a signal 2.5 standard deviations above the blank (zero) calibrator. Coefficient of variation values below 25% were accepted.

Proteomics

Homogenization of biopsy tissue before filter-aided sample preparation

Biopsies (n = 12/group) were processed for mass spectrometric analysis according to a filter-aided sample preparation protocol

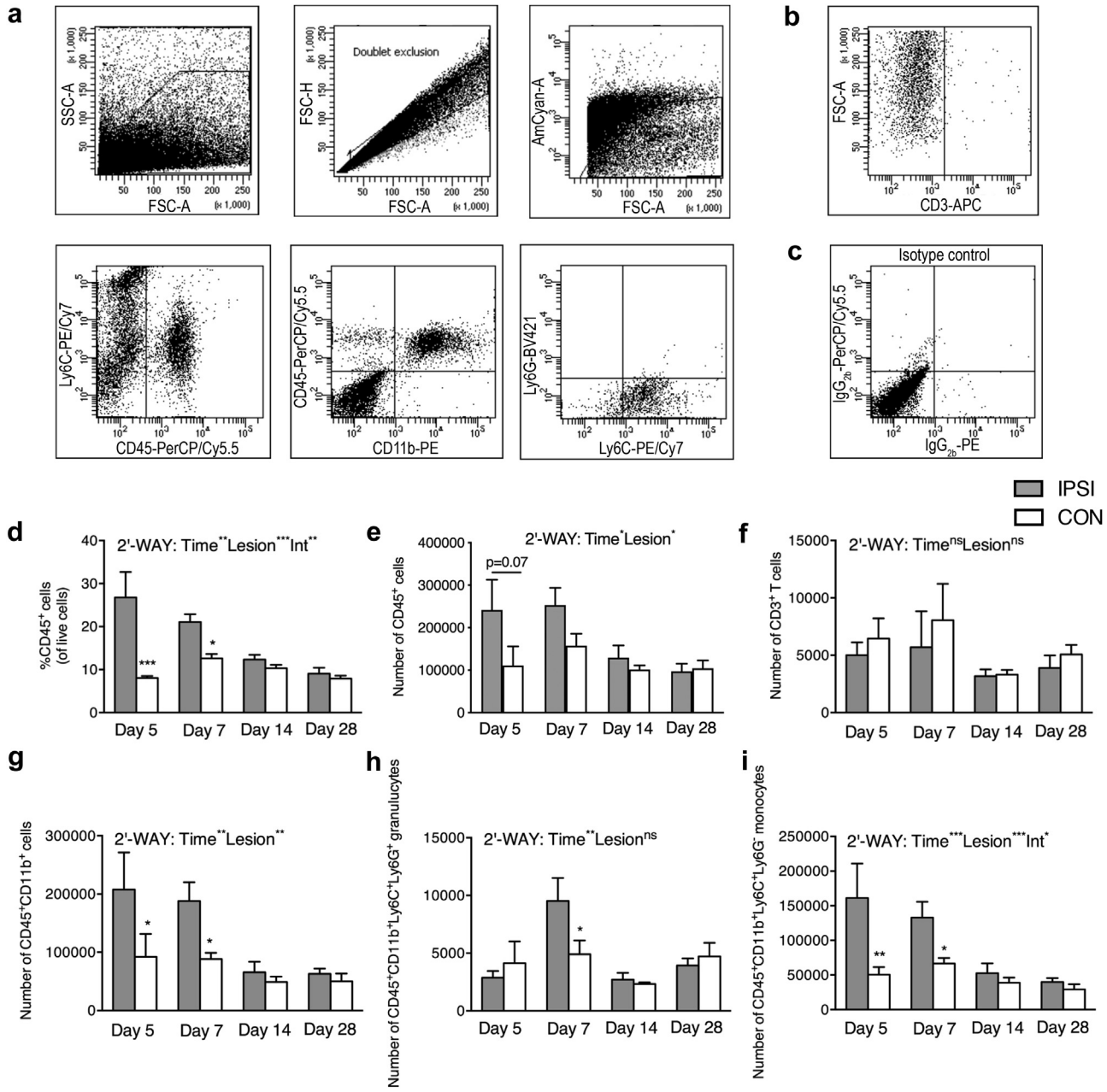

Figure 1 Flow cytometry analysis of inflammatory cells after experimental SS tendon tear. (**a**) Gating strategy: FSC/SSC was used to define cell populations. FSC/FSC was used to exclude duplets and only living cells were included. CD45 was used to define leukocytes and lymphocytes. CD45/CD11b was used to define leukocytes and Ly6G/Ly6C to differentiate between monocytes/macrophages and neutrophils. FSC/CD3 was used to define $CD45^+CD3^+$ T cells. (**b**) Representative isotype controls were used to assist gating. (**c**) $CD45^+$ cells populations were found be highest in the ipsilateral SS muscle at days 5 and 7 after SS tendon tear, decreasing over time (2-way ANOVA: lesion, $***P = .0002$, $F_{1,30} = 18.46$; time, $**P = .002$, $F_{1,30} = 6.06$; interaction, $**P = .008$, $F_{3,30} = 4.75$). At day 5 and day 7 (**d**), the percentage of $CD45^+$ cells was significantly increased in the ipsilateral SS muscle compared to the contralateral SS muscle ($P = .001$ and $P = .05$, respectively, Holm-Sidak multiple comparison test). (**e**) The total number of $CD45^+$ cells was found to be highest in the ipsilateral SS muscle at days 5 and 7, decreasing thereafter (2-way ANOVA: lesion, $*P = .016$, $F_{1,30} = 6.5$; time, $*P = .011$, $F_{3,30} = 4.38$; interaction, ns) with a tendency of significantly more $CD45^+$ cells in the ipsilateral SS muscle at day 5 compared to the contralateral SS muscle ($P = .07$, Holm-Sidak multiple comparison test day). (**f**) The number of $CD3^+$ T cells did not change over time and was similar between the ipsilateral and contralateral SS muscles. (**g**) The number of $CD45^+CD11b^+$ leukocytes was found be highest in the ipsilateral SS muscle at days 5 and 7 after SS tendon tear decreasing over time (2-way ANOVA: lesion, $**P = .0034$, $F_{1,30} = 10.12$; time, $**P = .0012$, $F_{3,30} = 6.87$; interaction, ns, followed by Holm-Sidak multiple comparison test day, $*P = .0375$). (**h**) The number of neutrophil granulocytes was significantly higher in the ipsilateral SS muscle compared to the contralateral SS muscle at day 7 ($*P = .0329$, Holm-Sidak multiple comparison test), whereas the number was comparable at all other time points investigated (2-way ANOVA: lesion, ns; time,

using bead beating for tissue lysis, reduction alkylation (tris(2-carboxyethyl)phosphine hydrochloride and carbonic anhydrase 5A; Sigma Aldrich) and trypsin (1:100; Promega Mass, Believe it is Wisconsin, USA) as protease.[6,7] The samples were stored at –80°C prior to ultraperformance liquid chromatography–tandem mass spectrometry (UPLC-MS/MS) analysis.

LC-MS/MS analysis

Each biopsy was analyzed in triplicate according to Bennike et al.[7] Essentially the samples were analyzed by LC-MS by Dionex RSLC Proflow nano-UPLC system connected to a Bruker timsTOF mass spectrometer (Bruker, Bremen, Germany). A pre-column setup (Acclaim PepMap100 C18 100 µm ID trap; 75 cm Acclaim Pepmap RSLC, 75 µm ID) was used. The buffers of the liquid chromatography system consisted of buffer A (0.1% FA) and buffer B (99.9% ACN, 0.1% FA) and an elution gradient from 5%-35% buffer B over 88 minutes. The mass spectrometer system was operated in data-dependent acquisition mode. Mass range of *m/z* 350-2200 was acquired at a resolution of approximately 45,000 for each full scan and up to 2 MS/MS acquisition of abundant peptide precursor ions in each cycle. Raw output data were identified using MaxQuant version 1.6.0.1 with Andromeda search engine against a reference proteome of mouse muscles (Proteome ID UP000000589, 16854 Entry).[38] Fixed modification was set with a carbamidomethylation. N-Terminal acetylation and oxidation of methionine was set as a variable modification.

To establish the cellular origin of the differentially expressed proteins in lesioned and nonlesioned muscle, the single-cell RNA expression in 2 muscle samples from healthy mice in the Panglao database (SRA653146:SRS3044258 and SRA851241:SRS4388159) was used.[14]

Statistical analysis

For comparison of grip strength, paired Student *t* test was applied. Estimation of the number of adipocytes over time was analyzed using 1-way analysis of variance (ANOVA) with Tukey post hoc test and multiple *t* test was used to compare ipsilateral vs contralateral SS muscles at any given time. For analysis of flow cytometry data, 2-way ANOVA with Holm-Sidak post hoc test was used. *P* values $\leq$.05 were accepted. Data are presented as mean $\pm$ standard deviation.

The proteomics search output, including label-free quantification data, was statistically filtered in Perseus.[38] Repeatability was evaluated by Pearson correlation in a range of >0.85 for technical replicates and sample groups. Identified protein groups were filtered using only label-free quantification values with 50% within 1 group and >2 unique peptides. Significant values were calculated based on a Student *t* test set with false discovery rate multiplicity adjustment with truncation (Permutation based false discovery rate [250 randomizations]), cutoff at 0.05, and an S0 value at 0.1. Significant values calculated for each protein were then plotted against the fold-change difference in protein expression between ipsilateral and contralateral SS muscle tissue (volcano plots). Principal components analysis was used to examine protein expression differences in the samples.

For functional classification of proteins, significant results were analyzed through the classification software PANTHER, version 13.1 (http://www.pantherdb.org). Bar plots were performed for results. Proteins were localized into functional groups based on Gene Ontology (GO) information. For the analysis of pathways and biological processes, Kyoto Encyclopedia of Genes and Genomes (KEGG) pathway and GO analysis were performed using ENRICHR.[10,27] String analysis was conducted using the STRING software, version 11.0.

Results

Experimental SS tendon tear impairs neuromuscular function

To validate if successful SS tendon cutting was obtained, we performed grip strength tests prior to and 5 days after SS tendon surgery. Prior to surgery, the grip strength was equivalent between the ipsilateral and contralateral front limbs ($P > .05$). Five days after SS tendon tear, the grip strength was significantly decreased on the ipsilateral front limb compared to the contralateral (ipsilateral: 77.60 $\pm$ 12.39 g and contralateral: 104.9 $\pm$ 11.95 g, $P = .0015$.

Muscle inflammation peaks 5 days after experimental SS tendon tear

For characterization of inflammation, we performed flow cytometry (Fig. 1). We estimated the percentage and number of $CD45^+$ cells (Fig. 1, *d* and *e*) and the number of T cells (Fig. 1, *f*), leukocytes (Fig. 1, *g*), neutrophils (Fig. 1, *h*), and macrophages (Fig. 1, *i*) in the ipsilateral and contralateral SS muscles at days 5, 7, 14, and 28 days after experimental SS tendon tear. The percentage of $CD45^+$ cells significantly increased in the ipsilateral compared to the contralateral SS at day 5 and 7 ($P = .001$ and $P = .05$, respectively; Fig. 1, *d*). $CD45^+$ cells appeared to reach peak values at days 5 and 7, declining thereafter (Fig. 1, *d* and *e*). The number of T cells was similar in the ipsilateral and contralateral SS muscles at all time points investigated (Fig. 1, *f*) and constituted only ~2% of the $CD45^+$ cells at day 5 and ~4% at day 28. The total number of leukocytes was significantly increased in the ipsilateral compared to the contralateral SS muscle at days 5 and 7 ($P = .0034$ and $P = .0012$), decreasing to comparable numbers at days 14

Fig. 1 *legend continues.* **$P = .0021$, $F_{3,28} = 6.32$; interaction, ns). (**i**) The total number of monocytes/macrophages was significantly increased in the ipsilateral SS muscle at days 5 and 7 (*$P = .0023$ and $P = .0439$, respectively, Holm-Sidak multiple comparison test), whereas the number decreased and was similar to the contralateral SS muscle (2-way ANOVA: lesion, ***$P = .0006$, $F_{1,30} = 14.50$; time, ***$P = .0006$, $F_{3,30} = 7.59$; interaction, *$P = .044$, $F_{3,30} = 3.05$). *$P < .05$, **$P < .01$. **$P < .001$ indicates significant differences between ipsilateral and contralateral SS muscles (n = 4-5/group). *FSC*, forward scatter; *SSC*, side scatter; *SS*, supraspinatus; *ns*, nonsignificant.

Table I Mean fluorescence intensity of CD11b and CD45 on neutrophils and macrophages

	Neutrophil CD11b expression		Macrophage CD11b expression		Neutrophil CD45 expression		Macrophage CD45 expression	
	Ipsilateral	Contralateral	Ipsilateral	Contralateral	Ipsilateral	Contralateral	Ipsilateral	Contralateral
Day 5	18,860 ± 7719	29,072 ± 39,769	11,260 ± 3515	9638 ± 2039	3783 ± 1295	3414 ± 3757	****2209 ± 178**	**1649 ± 136**
Day 7	6494 ± 935	9126 ± 4171	5149 ± 251	5601 ± 1052	2583 ± 368	4094 ± 2059	1997 ± 133	1807 ± 302
Day 14	6510 ± 4198	5506 ± 2716	6145 ± 885	6238 ± 983	4067 ± 3263	3841 ± 1621	1921 ± 82	1899 ± 237
Day 28	9065 ± 6290	7434 ± 3528	3566 ± 926	4056 ± 553	5200 ± 3909	13,511 ± 14,785	1540 ± 94	1829 ± 341

SS, supraspinatus.
N = 5 per group, except for contralateral SS in control and at day 5, where n = 4. Results are presented as mean ± standard deviation.
***P* < .01, comparison between ipsilateral and contralateral supraspinatus muscle.

and 28 (Fig. 1, *g*). The number of infiltrating neutrophils was significantly higher in the ipsilateral SS at day 7 compared to the contralateral ($P = .0021$), whereas no differences were observed at any other time point (Fig. 1, *h*). The total number of macrophages significantly increased in the ipsilateral compared to the contralateral SS muscle at both day 5 and 7 ($P = .0023$ and $P = .0439$ respectively), but with no significant difference between the sides at days 14 and 28 (Fig. 1, *i*).

Mean fluorescence intensity for CD11b on monocytes, CD11b, and CD45 on neutrophils was similar between ipsilateral and contralateral SS muscles at all time points investigated (Table I). CD45 expression on macrophages was, however, significantly increased at day 5 in the ipsilateral compared to the contralateral SS (Table I).

Experimental SS tendon tear leads to significant changes in cytokine levels in the SS muscle

We next investigated potential changes in several pro- and anti-inflammatory cytokines (Fig. 2, *i*). We found that the cytokines IL-10, TNF, IL-4, IL-5, IL-1β, IL-6, and CXCL1 were significantly increased at day 5 in the ipsilateral compared with the contralateral SS muscle (Fig. 2, *i*).

Experimental SS tendon tear leads to changes in proteins related to inflammation, degeneration and regeneration in the SS muscle

Proteomic analysis revealed 156 proteins out of a total of 205 detected proteins to be differentially expressed between the ipsilateral and contralateral SS muscles 5 days after SS tendon tear (Supplementary Table S1). Of these, 133 proteins were significantly upregulated, and 23 proteins were significantly downregulated in the ipsilateral SS (Supplementary Table S1).

Among the downregulated proteins particularly expressed in muscle fibers were Kelch-like protein 31 and 41 and fructose-1, 6-bisphosphatase isozyme 2, whereas neonatal myosin (Myh8) was upregulated. This demonstrated an early indication of muscle atrophy in the lesioned muscle.

GO analysis on biological processes showed that upregulated proteins (Supplementary Figure S1 and Supplementary Table S2) generally were included in pathways different from those involving the downregulated (Supplementary Figure S2, *a*, and Supplementary Table S2). GO analysis of the 23 proteins downregulated in the ipsilateral SS muscle resulted in 33 pathways with an adjusted *P* value lower than .05 (Supplementary Table S2). String analysis based on KEGG mouse pathway of upregulated proteins revealed 4 clusters of differentially expressed proteins (Fig. 2, *a*) and downregulated proteins revealed 2 clusters of differentially expressed proteins (Supplementary Figure S2, *b*). The clusters of upregulated

proteins included proteins involved in the regulation of the actin cytoskeleton, ECM receptor interaction, and protein processing in the endoplasmic reticulum, and complement and coagulation cascades. This was supported by GO analysis (Supplementary Table S1), which revealed that the majority of the significantly changed pathways were related to proteins involved in ''Neutrophil activation involved in immune response'' (Fig. 2, *b*), ''Cellular response to interleukin-12'' (Fig. 2, *c*), ''Regulation of lipid biosynthetic process'' (Fig. 2, *d*), ''Extracellular matrix organization'' (Fig. 2, *e*), ''Skeletal muscle tissue development and contraction'' (Fig. 2, *f*), and ''Respiratory electron transport chain'' (Fig. 2, *g*).

To establish the cellular origin of the proteins, the clusters of single cells expressing the RNA corresponding to the proteins were found in the Panglao database in murine muscle.

The genes involved in the pathway ''Extracellular matrix organization'' were all expressed in FAPs except *Lcp1, which was expressed in macrophages and lymphocytes* (Supplementary Table S1). *Interestingly, most of the genes were differently expressed in subpopulations of FAPs. C4b, Col14a1, Pygl, A2m, and Col5a1 were found mainly in 1 cluster, whereas Tnc, Thbs4, Col1a1, and Clu were expressed in the remaining FAPs.*

Collagen accumulates in the ipsilateral SS muscle after experimental SS tendon tear

Sirius Red stain (Fig. 3) showed a continuous increase of interstitial collagen in the lesioned side during the study (Fig. 3, *c*). Collagen accumulation in the contralateral muscle was absent until day 28, when we observed a minor increase (not shown).

Adipocytes develop in the SS muscle after experimental SS tendon tear

Countings from parallel Oil Red O–, hematoxylin-eosin–, and Sirius Red–stained SS muscle sections (Fig. 4, *a* through *f*) after RC tendon tear showed that the number of adipocytes was low during the first 7 days; however, at day 14, an increased number of adipocytes was observed (Fig. 4, *g*). The same tendency was observed at day 28, where we found an increased number of adipocytes in the ipsilateral compared to the contralateral SS.

Regenerative niche in the SS muscle after experimental SS tendon tear

To investigate the regenerative niche in the SS muscle after SS tendon tear, we performed flow cytometry analysis and gated on satellite cells (Fig. 5). Gating was performed to include $CD45^{-}CD31^{-}Sca1^{-}Integrin\text{-}\alpha7^{+}$ satellite cells[29] (Fig. 5, *a* and *b*). We estimated the percentage (Fig. 5, *c*) and total number (Fig. 5, *f*) of $CD45^{-}$ cells in SS muscle bilaterally at days 5, 7, 14, and 28 after SS tendon tear. The population of $CD45^{-}$ cells increased over time, and we saw a significantly higher percentage of $CD45^{-}$ cells in the contralateral SS at day 5 and 7 compared with the ipsilateral SS muscle ($P = .001$ and $P = .05$, respectively; Fig. 5, *f*). The percentage of satellite cells in relation to $CD45^{-}$ cells decreased over time both in the lesioned and nonlesioned side, though the absolute numbers of satellite cells increased over time (Fig. 5, *g*). Interestingly, the increase in total number of satellite cells was significantly higher in the nonoperated SS muscle at all time points (Fig. 5, *d*).

It was not possible to establish a uniform gating based on CD31 expression that could separate $CD45^{-}Sca1^{+}CD31^{+}$ endothelial cells and $CD45^{-}Sca1^{+}CD31^{-}$ FAPs. The percentage of $Sca1^{+}$ cells decreased from day 7 to day 14 and stayed at this level until day 28; however, the absolute number of $Sca1^{+}$ cells increased from day 5 to day 7 and stayed at this level throughout the study period (Fig. 5, *e* and *h*).

Discussion

The most widely reported consequences of RC tendon tear repair is poor tendon healing[18] that is associated with RC muscle fiber atrophy and fat accumulation in and around muscle fibers.[17,32] The present study provides evidence of early, time-dependent activation of inflammatory mediators during muscle adaptation to experimental SS tendon tear.

We observed an increase in inflammatory cells including neutrophils and monocytes/macrophages at days 5-7. In support of this, ''Neutrophil activation involved in immune response'' was one of the most enriched pathways in our proteomics analyses. Our results also demonstrated similar neutrophil numbers between ipsilateral and contralateral SS muscles, except at day 7. The inflammatory response peaked around days 5-7 and was mainly driven by macrophages with the highest CD45 mean fluorescence intensity at day 5. This showed increased macrophage activation at this time point. Similar to studies of mechanically induced muscle injury, these findings support a peak in the inflammatory response of the muscle around day 5 following the experimental tendon tear, whereafter the inflammatory response gradually resolved.[3,22]

Protein analysis of SS muscles 5 days after RC tendon tear demonstrated that the protein abundances of the complement proteins C3 and Cfb were significantly increased in the ipsilateral SS muscle, suggesting that the alternative complement activation pathway is involved in SS muscle inflammatory processes that follow RC tendon tear. Complement C3a signaling has also previously been shown to facilitate skeletal muscle regeneration by regulating monocyte function and trafficking following cardiotoxin-induced muscle injury in mice.[44] Proinflammatory monocytes recruited from the blood into injured muscle function as phagocytes and are rapidly converted to anti-

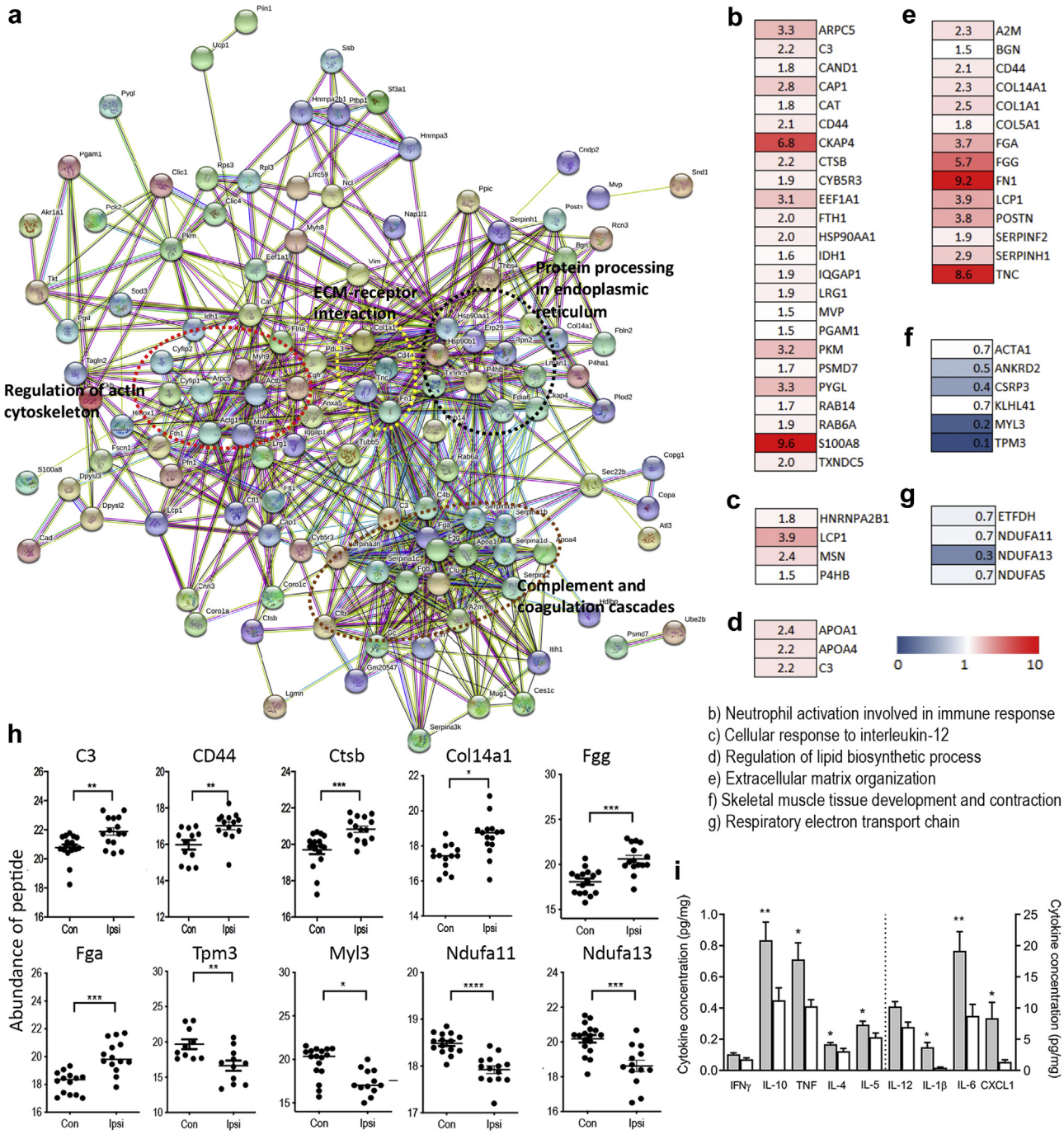

Figure 2 Proteome and cytokine analysis of ipsilateral and contralateral SS muscles 5 days after experimental SS tendon tear. (**a**) String analysis of differentially expressed proteins in ipsilateral and contralateral SS muscles 5 days post-surgery. (**b-g**) Levels of upregulated (red) or downregulated (blue) proteins involved in neutrophil activation involved in immune response (**b**), cellular response to interleukin-12 (**c**), regulation of lipid biosynthesis process (**d**), extracellular matrix organization (**e**), skeletal muscle tissue development and contraction (**f**), and respiratory electron transport chain (**g**) as measured by proteomics (n = 12 muscles per group). (**h**) Protein expression profiles of significantly altered, selected proteins in ipsilateral and contralateral SS muscles 5 days postsurgery. Dot plot represents number of spectral matches of each unique peptide providing evidence for the identification of the abundance of a peptide for a given protein. (**i**) Multiplex analysis of inflammatory cytokines 5 days post-surgery in ipsilateral and contralateral SS muscles (n = 8/group). *P* values for IFNγ = 0.3111, IL-1β = 0.0122, IL-2 = 0.3206, IL-4 = 0.0471, IL-5 = 0.0153, IL-6 = 0.0041, IL-10 = 0.0081, IL-12 = 0.0563, CXCL1 = 0.0238, and TNF = 0.0116, paired Student *t* test. *A2M*, alpha-2-macroglobulin; *ACTA1*, actin, alpha skeletal muscle; *ANKRD2*, ankyrin repeat domain-containing protein 2; *APOA1*, apolipoprotein A-I; *APOA4*, apolipoprotein A-IV; *ARPC5*, actin-related protein 2/3 complex subunit 5; *BGN*, biglycan; *C3*, complement C3; *CAND1*, cullin-associated NEDD8-dissociated protein 1; *CAP1*, adenylyl cyclase-associated protein 1; *CAT*, catalase; *CD44*, CD44 antigen; *CKAP4*, cytoskeleton-associated protein 4; *COL14A1*, collagen alpha-1(XIV)

inflammatory macrophages that promote the proliferation and differentiation of satellite cells.[3] In the present study, we found the number of macrophages to be highest in the ipsilateral SS muscle at day 5, where also proinflammatory cytokine levels were higher compared with the contralateral SS muscle. Altogether, these results, supported by STRING analysis, suggest a muscle regenerative potential at day 5.

We observed an increase in collagen accumulation between the muscle fibers and a change in collagen accumulation near the musculotendinous junction from day 14. In addition, we observed increased fatty infiltration from day 14 and onward. This is in line with a recent study in rabbits also demonstrating fatty infiltration of the SS muscle 14 days after experimental RC tear.[1] Similar or even more pronounced fatty infiltration was reported from animal models based on the creation of a massive RC tendon tear in combination with denervation of the muscles.[11,31,32] Such massive torn and denervated RC muscle is, however, clinically less relevant without repair options.

In patients with traumatic RC tendon tear, we previously demonstrated SS muscle inflammation combined with fatty infiltration and degeneration.[16] Both in that study and in the present study, we observed significant changes in proteins involved in lipid metabolism (humans: APOA1, APOA4, EEF1A2, PLIN1, and SLC25A1; mice: EEF1A1 and SLC5A5), ECM (humans: COL5A3; mice: COL1A1, COL4A1, and COL5A1), and muscle structure development (humans: ANKRD2, MYL3, MYH3, MYH7, NDUFA4, and BDUFA9; mice: MYH8, MYH9, NDUFA5, NDUFA11, and NDUFA13), suggesting similar pathophysiological changes in humans and mice under tear conditions. This is further supported by previous studies demonstrating significant inflammatory changes in the SS muscle in both mouse[37] and rat[23] subjected to RC tendon tear with denervation of the suprascapular nerve. As late as 1 month after surgery in mice, Talarek et al[37] observed significant changes in gene expression levels for some of the same proteins that we found upregulated already 5 days after RC tendon tear. The same was true in rats 10, 30, and 60 days after tendon tear.[23] The genes and proteins altered were found to be involved in inflammation (*il1b*, *il6*), ECM (*Bgn*, *ColaA1*, *Col14A1*, *Thbs4*, *Tnc*), muscle atrophy (*Ctsb*, *Eef1a1*), muscle fiber contractility and cytoskeletal organization (*Acta1*, *Msn*, *Myh8*), and muscle metabolism (*Fbp2*, *Pkm*, *Plin1*, *Thbs4*). Based on this, we therefore suggest that SS tendon tear is accompanied by changes in a wide range of inflammatory markers important for the regenerative potential of the SS muscle.

The number of satellite cells in both sides increased from day 5 to day 7. At all time points, the number of satellite cells was higher in the nonoperated side. The increase of satellite cells in the contralateral muscle could be explained by increased load on the healthy leg because these cells are activated by physical activity. The increase in the ipsilateral SS muscle could be a result of the tendon lesion. Davies et al[13] investigated muscle stem cell activation 3, 8, or 14 weeks after SS and infraspinatus tendon tear in mice and demonstrated that muscle stem cells were transiently activated and not depleted, in spite of persistent muscle atrophy.

Besides satellite cells, other cell types are believed to contribute to the process of muscle regeneration.[41] Among these cell types are endothelial cells and FAPs. The number of these cells increased from day 5. Considering that inactivation of a skeletal muscle results in a rapid reduction in capillarization,[25] the FAPs most likely account for our observed increase in $Sca1^+$ cells in the ipsilateral side. In the contralateral muscle, an increase in both endothelial cells and FAPs is likely a consequence of increased load. The development of fatty infiltration and fibrosis in the lesioned side, together with upregulation of genes involved in lipid and ECM metabolism, indicate that some FAPs here depart from their muscle-supporting activity and develop into adipocytes and fibroblasts. On the contralateral side, the $Sca1^+$ cells more likely support the myogenic cells. The apparently differential expression of proteins in FAPs on the 2 sides supports the suggestion of such a functional difference.

One limitation in the present study is that our model is not able to distinguish between chronic disease and acute inflammation. However, the purpose of this study was to examine the acute muscle inflammatory reactions believed also to occur in patients with traumatic RC tendon tears. The elucidation of the time-dependent inflammatory, degenerative, and regenerative responses of the SS muscle in tear conditions could pave the way for timely

Fig. 2 *legend continues.* chain; *COL1A1*, collagen alpha-1(I) chain; *COL5A1*, collagen alpha-1(V) chain; *CSRP3*, cysteine and glycine-rich protein 3; *CTSB*, cathepsin B; *CYB5R3*, NADH-cytochrome b5 reductase 3; *EEF1A1*, elongation factor 1-alpha 1; *ETFDH*, electron transfer flavoprotein-ubiquinon oxidoreductase, mitochondrial; *FGA*, fibrinogen alpha chain; *FGG*, fibrinogen gamma chain; *FN1*, profilin-1; *FTH1*, ferritin heavy chain; *HNRNPA2B1*, heterogeneous nuclear ribonucleoproteins A2/B1; *HSP90AA1*, heat shock protein HSP 90-alpha; *IDH1*, isocitrate dehydrogenase [NADP] cytoplasmic; *IQGAP1*, ras GTPase-activating-like protein; *KLHL41*, kelch-like protein 41; *LCP1*, plastin-2; *LRG1*, leucine-rich alpha-2-glycoprotein 1; *MSN*, moesin; *MVP*, major vault protein; *MYL3*, myosin light chain 3; *NDUFA11*, NADH dehydrogenase [ubiquinone] alpha subcomplex subunit 11; *NDUFA13*, NADH dehydrogenase [ubiquinone] alpha subcomplex subunit 13; *NDUFA5*, NADH dehydrogenase [ubiquinone] alpha subcomplex subunit 5; *P4HB*, protein disulfide-isomerase; *PGAM1*, phosphoglycerate mutase 1; *PKM*, pyruvate kinase; *POSTN*, periostin; *PSMD7*, 26S proteasome non-APTase regulatory subunit 7; *PYGL*, glycogen phosphorylase; *RAB14*, ras-related protein rab-14; *RAB6A*, ras-related protein rab-6A; *S100A8*, protein S100-A8; *SERPINF2*, alpha-2 antiplasmin; *SERPINH1*, serpin H1; *TNC*, tenascin; *TPM3*, tropomyosin alpha-3 chain; *TXNDC5*, thioredoxin domain-containing protein 5.

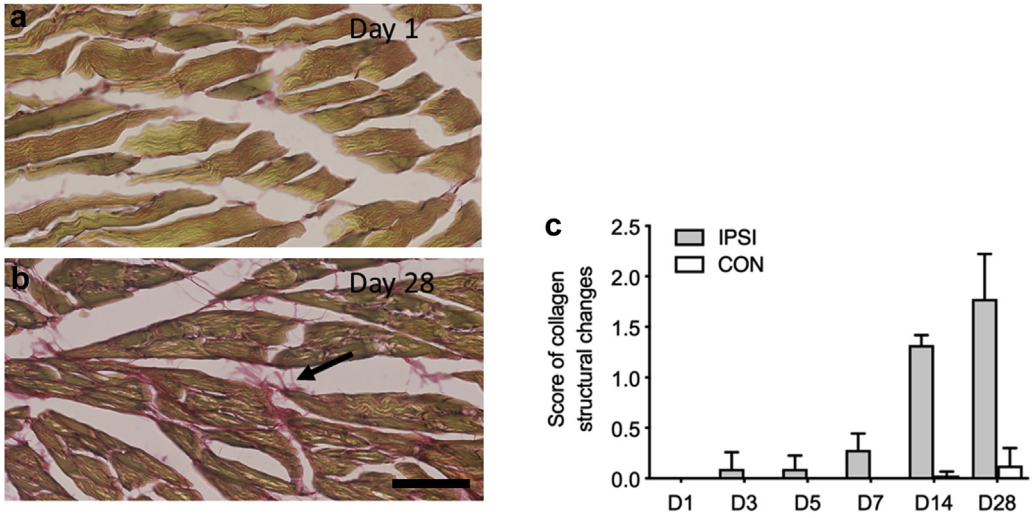

Figure 3 Sirius Red staining of SS muscle after experimental SS tendon tear. (**a**,**b**) Representative Sirius Red–stained sections of the SS muscle from (**a**) 1 day and (**b**) 28 days postsurgery. The arrow points at collagen in the interstitium. Scale bar: 50 μm. (**c**) Scoring of Sirius Red–stained tissue sections demonstrating increased collagen accumulation 14 and 28 days postsurgery.

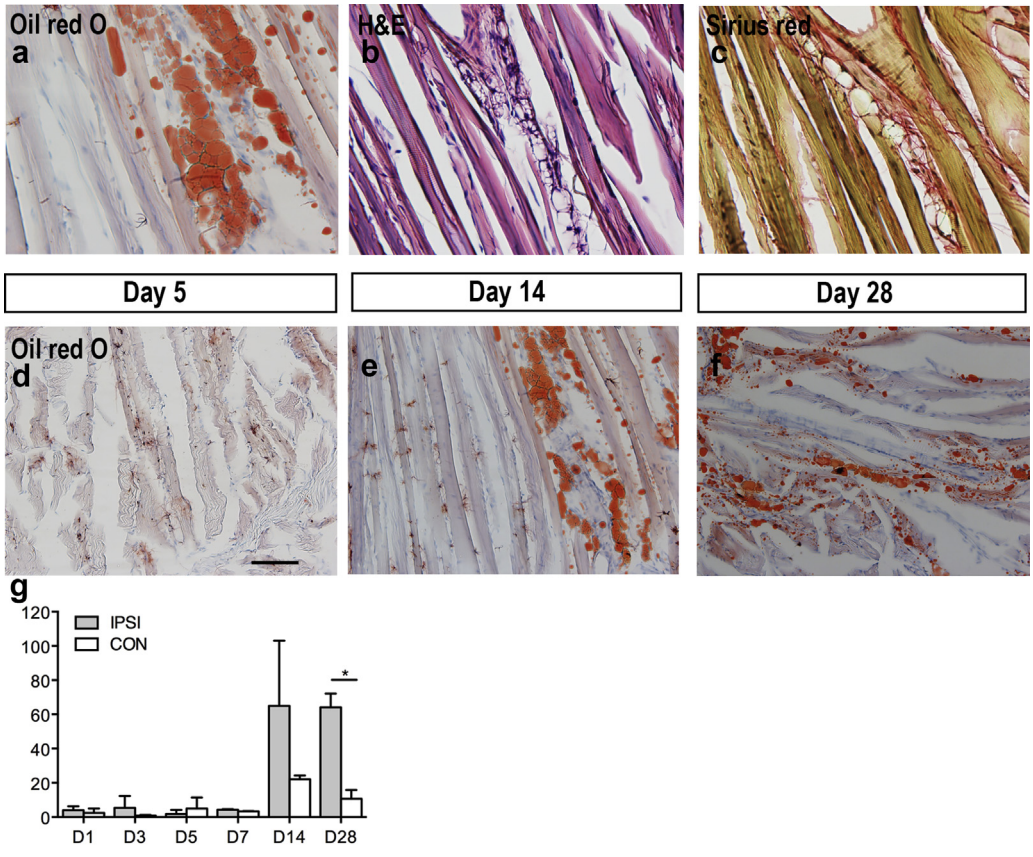

Figure 4 Fatty infiltration of the SS muscle after experimental SS tendon tear. (**a-c**) The morphology 14 days post-surgery of adipocytes in (**a**) Oil red O, (**b**) hematoxylin-eosin, and (**c**) Sirius Red muscle stained in parallel sections from an ipsilateral SS muscle. Scale bar: 50 μm (**d-f**) Oil red O–stained tissue sections 5 days (**d**), 14 days (**e**), and 28 days (**f**) postsurgery in the ipsilateral SS muscle. Scale bar: 100 μm. (**g**) Total number of adipocytes estimated in Oil red O–stained tissue sections demonstrating significantly increased fatty infiltration 28 days postsurgery in the ipsilateral compared to the contralateral SS muscle (multiple *t* test). $*P = .0015$.

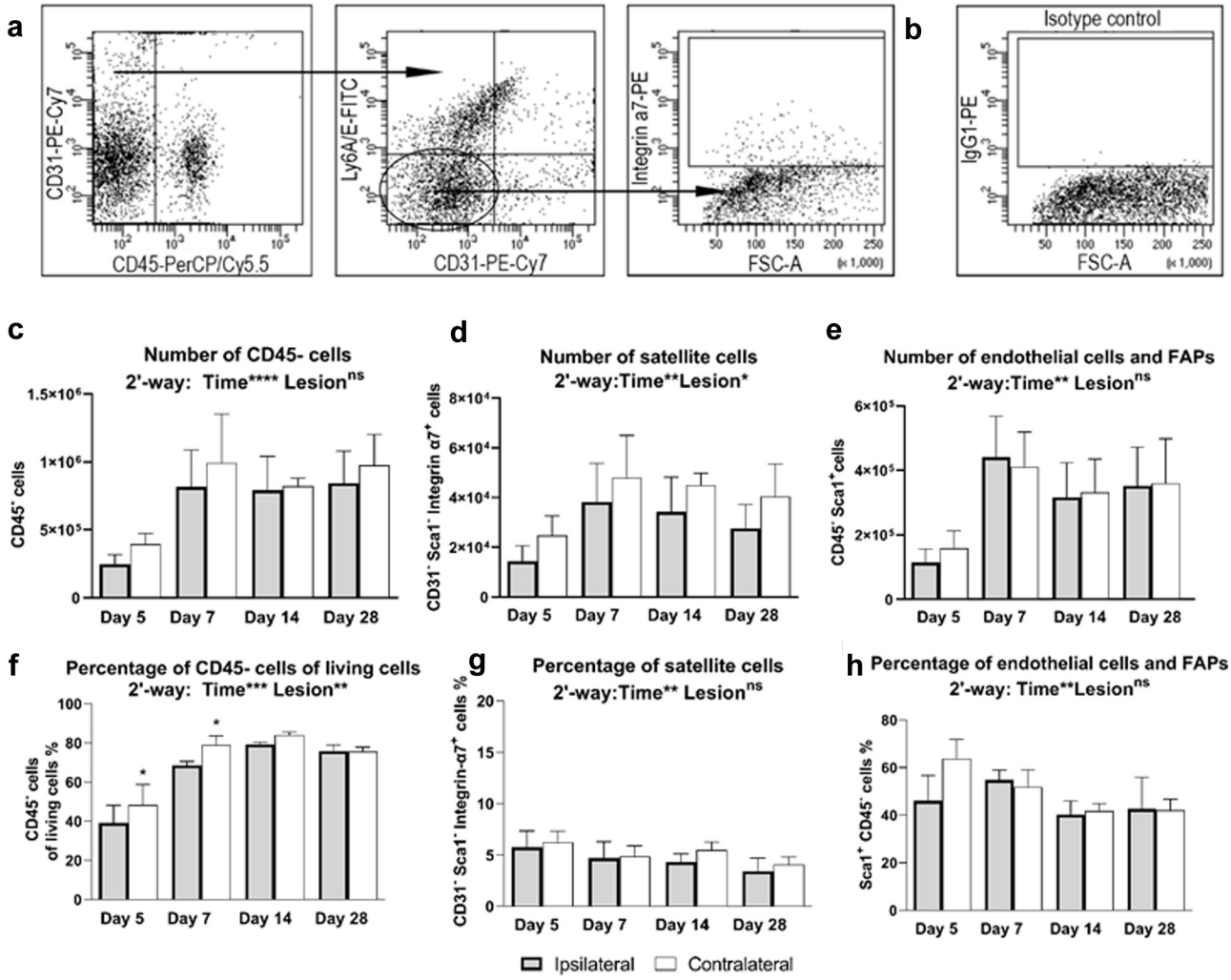

Figure 5 Flow cytometry analysis of muscle stem cells after experimental SS tendon tear. (**a**) Gating strategy. CD31/CD45 was used to define $CD45^-$ cells in order to exclude leukocytes and lymphocytes. CD31/Ly6A/E (Sca-1) was then used to exclude $CD31^+$ endothelial cells and $Ly6A/E^+$ hematopoietic stem cells. Finally, FSC-A and integrin-α7 were used to define skeletal muscle satellite cells. (**b**) Isotype control for integrin-α7. (**c**) The total number of $CD45^-$ cells significantly increased from day 5 and onward with no significant difference between the ipsilateral and contralateral SS muscles (2-way ANOVA: lesion, ns; time, $****P < .001$, $F_{3,32} = 16.33$; interaction, ns). (**d**) The total number of integrin-$\alpha7^+$ satellite cells increased over time demonstrating increased numbers of satellite cells in the contralateral SS muscle at all time points (2-way ANOVA: lesion, $*P = .02$, $F_{1,32} = 6.17$; time, $**P = .001$, $F_{3,32} = 6.84$; interaction, ns). (**e**) The total number of endothelial cells and FAPs increased over time (2-way ANOVA: lesion, ns; time, $**P = .0016$, $F_{3,16} = 8.193$; interaction, ns). (**f**) The percentage of $CD45^-$ cells increased over time (2-way ANOVA: lesion, $**P = .0012$, $F_{1,32} = 12.67$; time, $***P < .001$, $F_{3,32} = 99.47$; interaction, ns), with a significantly increased proportion of $CD45^-$ cells in the contralateral SS muscle compared to the ipsilateral SS muscle at days 5 and 7 ($*P < .0001$ for both), Holm-Sidak multiple comparison test day). (**g**) The percentage of integrin-$\alpha7^+$ satellite cells significantly decreased over time with no significant difference between the ipsilateral and contralateral SS muscles (2-way ANOVA: lesion, ns; time, $**P = .0013$, $F_{3,32} = 6.61$; interaction, ns). (**h**) The percentage of endothelial cells and FAPs changed over time (2-way ANOVA: time, $**P = .0017$, $F_{3,16} = 8.022$). $*P < .05$, $**P < .01$, $**P < .001$ (n = 4-5/group). *FAPs*, fibro-adipogenic progenitors; *FSC*, forward scatter; *SSC*, side scatter; *SS*, supraspinatus; *ANOVA*, analysis of variance.

intervention in patients with RC tears. This model of acute tendon resection does not therefore perfectly replicate the chronic degenerative process of RC tears often seen in humans.

In the present study, we used proteomics to detect changes in proteins between the ipsilateral and contralateral SS muscle 5 days after tendon tear. A limitation of proteomics is that this method cannot be used to detect low molecular weight proteins, such as cytokines, chemokines, and growth factors.

Another limitation of the present study is the lack of validated scoring systems for our histologic analyses. Histologic scores, however, were established in collaboration with a

pathologist specialized in muscle diseases, sections were blinded, and compared to nonlesioned contralateral muscle.

Conclusion

Our study revealed substantial SS muscle responses within the first 4 weeks after experimental SS tendon tear, allowing us to study the time-dependent inflammatory impact on degeneration and regeneration of the SS muscle. Inflammation peaked at days 5-7, followed by a gradual decrease. Fibrosis and fatty infiltration prevailed from day 14, as did FAPs, and despite an early increase in satellite cell numbers and several factors in favor of regeneration, the potential of the detached SS muscle to this response appeared to be inferior. Ultimately, understanding the relationship between inflammation and regenerative capacity and disease state will aid in identifying the proper intervention of the individual patient with RC tendon tear.

Disclaimers:

Funding: This work was supported by generous funding from Fonden til Lægevidenskabens Fremme–AP Møller Fonden.
Conflicts of Interest: Kate Lykke Lambertsen is a member of the Brain Prize Council at the Lundbeck Foundation. All the other authors, their immediate families, and any research foundations with which they are affiliated have not received any financial payments or other benefits from any commercial entity related to the subject of this article.

Acknowledgments

Ulla Damgaard Munk and Anni Petersen are acknowledged for skilled technical assistance.

Supplementary data

Supplementary data to this article can be found online at https://doi.org/10.1016/j.jse.2021.12.046.

References

1. Abdou MA, Kim GE, Kim J, Kim BH, Kim YK, Jeong SE, et al. How long should we wait to create the Goutallier stage 2 fatty infiltrations in the rabbit shoulder for repairable rotator cuff tear model? Biomed Res Int 2019;2019:7387131. https://doi.org/10.1155/2019/7387131
2. Andersen DC, Laborda J, Baladron V, Kassem M, Sheikh SP, Jensen CH. Dual role of delta-like 1 homolog (DLK1) in skeletal muscle development and adult muscle regeneration. Development 2013;140:3743-53. https://doi.org/10.1242/dev.095810
3. Arnold L, Henry A, Poron F, Baba-Amer Y, van Rooijen N, Plonquet A, et al. Inflammatory monocytes recruited after skeletal muscle injury switch into antiinflammatory macrophages to support myogenesis. J Exp Med 2007;204:1057-69. https://doi.org/10.1084/jem.20070075
4. Barry JJ, Lansdown DA, Cheung S, Feeley BT, Ma CB. The relationship between tear severity, fatty infiltration, and muscle atrophy in the supraspinatus. J Shoulder Elbow Surg 2013;22:18-25. https://doi.org/10.1016/j.jse.2011.12.014
5. Bell R, Taub P, Cagle P, Flatow EL, Andarawis-Puri N. Development of a mouse model of supraspinatus tendon insertion site healing. J Orthop Res 2015;33:25-32. https://doi.org/10.1002/jor.22727
6. Bennike TB, Ellingsen T, Glerup H, Bonderup OK, Carlsen TG, Meyer MK, et al. Proteome analysis of rheumatoid arthritis gut mucosa. J Proteome Res 2017;16:346-54. https://doi.org/10.1021/acs.jproteome.6b00598
7. Bennike TB, Kastaniegaard K, Padurariu S, Gaihede M, Birkelund S, Andersen V, et al. Comparing the proteome of snap frozen, RNAlater preserved, and formalin-fixed paraffin-embedded human tissue samples. EuPA Open Proteom 2016;10:9-18. https://doi.org/10.1016/j.euprot.2015.10.001
8. Benson RT, McDonnell SM, Knowles HJ, Rees JL, Carr AJ, Hulley PA. Tendinopathy and tears of the rotator cuff are associated with hypoxia and apoptosis. J Bone Joint Surg Br 2010;92:448-53. https://doi.org/10.1302/0301-620x.92b3.23074
9. Brioche T, Pagano AF, Py G, Chopard A. Muscle wasting and aging: experimental models, fatty infiltrations, and prevention. Mol Aspects Med 2016;50:56-87. https://doi.org/10.1016/j.mam.2016.04.006
10. Chen EY, Tan CM, Kou Y, Duan Q, Wang Z, Meirelles GV, et al. Enrichr: interactive and collaborative HTML5 gene list enrichment analysis tool. BMC Bioinformatics 2013;14:128. https://doi.org/10.1186/1471-2105-14-128
11. Cho E, Zhang Y, Pruznak A, Kim HM. Effect of tamoxifen on fatty degeneration and atrophy of rotator cuff muscles in chronic rotator cuff tear: An animal model study. J Orthop Res 2015;33:1846-53. https://doi.org/10.1002/jor.22964
12. Clausen BH, Degn M, Sivasaravanaparan M, Fogtmann T, Andersen MG, Trojanowsky MD, et al. Conditional ablation of myeloid TNF increases lesion volume after experimental stroke in mice, possibly via altered ERK1/2 signaling. Sci Rep 2016;6:29291. https://doi.org/10.1038/srep29291
13. Davies MR, Garcia S, Tamaki S, Liu X, Lee S, Jose A, et al. Muscle stem cell activation in a mouse model of rotator cuff injury. J Orthop Res 2018;36:1370-6. https://doi.org/10.1002/jor.23679
14. Franzén O, Gan LM, Björkegren JLM. PanglaoDB: a web server for exploration of mouse and human single-cell RNA sequencing data. Database (Oxford) 2019;2019:baz046. https://doi.org/10.1093/database/baz046
15. Freygant M, Dziurzynska-Bialek E, Guz W, Samojedny A, Golofit A, Kostkiewicz A, et al. Magnetic resonance imaging of rotator cuff tears in shoulder impingement syndrome. Pol J Radiol 2014;79:391-7. https://doi.org/10.12659/PJR.890541
16. Frich LH, Fernandes LR, Schroder HD, Hejbol EK, Nielsen PV, Jorgensen PH, et al. The inflammatory response of the supraspinatus muscle in rotator cuff tear conditions. J Shoulder Elbow Surg 2021;30:e261-75. https://doi.org/10.1016/j.jse.2020.08.028
17. Gibbons MC, Singh A, Anakwenze O, Cheng T, Pomerantz M, Schenk S, et al. Histological evidence of muscle degeneration in advanced human rotator cuff disease. J Bone Joint Surg Am 2017;99:190-9. https://doi.org/10.2106/JBJS.16.00335
18. Gladstone JN, Bishop JY, Lo IK, Flatow EL. Fatty infiltration and atrophy of the rotator cuff do not improve after rotator cuff repair and correlate with poor functional outcome. Am J Sports Med 2007;35:719-28. https://doi.org/10.1177/0363546506297539

19. Gokmen D, Ozkan K, Ali T, Ferhat G, Adil T. Fatty degeneration and atrophy of the rotator cuff muscles after arthroscopic repair: does it improve, halt or deteriorate? Arch Orthop Trauma Surg 2014 Jul; 134(7):985-90. https://doi.org/10.1007/s00402-014-2009-5
20. Godeneche A, Elia F, Kempf JF, Nich C, Berhouet J, Saffarini M, et al. Fatty infiltration of stage 1 or higher significantly compromises long-term healing of supraspinatus repairs. J Shoulder Elbow Surg 2017;26: 1818-25. https://doi.org/10.1016/j.jse.2017.03.024
21. Greenspoon JA, Petri M, Warth RJ, Millett PJ. Massive rotator cuff tears: pathomechanics, current treatment options, and clinical outcomes. J Shoulder Elbow Surg 2015;24:1493-505. https://doi.org/10.1016/j.jse.2015.04.005
22. Gumucio J, Flood M, Harning J, Phan A, Roche S, Lynch E, et al. T lymphocytes are not required for the development of fatty degeneration after rotator cuff tear. Bone Joint Res 2014;3:262-72. https://doi.org/10.1302/2046-3758.39.2000294
23. Gumucio JP, Qasawa AH, Ferrara PJ, Malik AN, Funai K, McDonagh B, et al. Reduced mitochondrial lipid oxidation leads to fat accumulation in myosteatosis. FASEB J 2019;33:7863-81. https://doi.org/10.1096/fj.201802457RR
24. Hamrick MW, McGee-Lawrence ME, Frechette DM. Fatty infiltration of skeletal muscle: mechanisms and comparisons with bone marrow adiposity. Front Endocrinol (Lausanne) 2016;7:69. https://doi.org/10.3389/fendo.2016.00069
25. Kanazashi M, Tanaka M, Maezawa T, Fujino H. Effects of reloading after chronic neuromuscular inactivity on the three-dimensional capillary architecture in rat soleus muscle. Acta Histochem 2020; 122:151617. https://doi.org/10.1016/j.acthis.2020.151617
26. Kuenzler MB, Nuss K, Karol A, Schar MO, Hottiger M, Raniga S, et al. Neer Award 2016: reduced muscle degeneration and decreased fatty infiltration after rotator cuff tear in a poly(ADP-ribose) polymerase 1 (PARP-1) knock-out mouse model. J Shoulder Elbow Surg 2017;26:733-44. https://doi.org/10.1016/j.jse.2016.11.009
27. Kuleshov MV, Jones MR, Rouillard AD, Fernandez NF, Duan Q, Wang Z, et al. Enrichr: a comprehensive gene set enrichment analysis web server 2016 update. Nucleic Acids Res 2016;44:W90-7. https://doi.org/10.1093/nar/gkw377
28. Madsen PM, Clausen BH, Degn M, Thyssen S, Kristensen LK, Svensson M, et al. Genetic ablation of soluble tumor necrosis factor with preservation of membrane tumor necrosis factor is associated with neuroprotection after focal cerebral ischemia. J Cereb Blood Flow Metab 2016;36:1553-69. https://doi.org/10.1177/0271678X15610339
29. Maesner CC, Almada AE, Wagers AJ. Established cell surface markers efficiently isolate highly overlapping populations of skeletal muscle satellite cells by fluorescence-activated cell sorting. Skelet Muscle 2016;6:35. https://doi.org/10.1186/s13395-016-0106-6
30. Matthews TJ, Hand GC, Rees JL, Athanasou NA, Carr AJ. Pathology of the torn rotator cuff tendon. Reduction in potential for repair as tear size increases. J Bone Joint Surg Br 2006;88:489-95. https://doi.org/10.1302/0301-620x.88b4.16845
31. Meyer DC, Hoppeler H, von Rechenberg B, Gerber C. A pathomechanical concept explains muscle loss and fatty muscular changes following surgical tendon release. J Orthop Res 2004;22:1004-7. https://doi.org/10.1016/j.orthres.2004.02.009
32. Rubino LJ, Stills HF Jr, Sprott DC, Crosby LA. Fatty infiltration of the torn rotator cuff worsens over time in a rabbit model. Arthroscopy 2007;23:717-22. https://doi.org/10.1016/j.arthro.2007.01.023
33. Schmutz S, Fuchs T, Regenfelder F, Steinmann P, Zumstein M, Fuchs B. Expression of atrophy mRNA relates to tendon tear size in supraspinatus muscle. Clin Orthop Relat Res 2009;467:457-64. https://doi.org/10.1007/s11999-008-0565-0
34. Schubert MF, Noah AC, Bedi A, Gumucio JP, Mendias CL. Reduced myogenic and increased adipogenic differentiation capacity of rotator cuff muscle stem cells. J Bone Joint Surg Am 2019;101:228-38. https://doi.org/10.2106/JBJS.18.00509
35. Shen H, Lim C, Schwartz AG, Andreev-Andrievskiy A, Deymier AC, Thomopoulos S. Effects of spaceflight on the muscles of the murine shoulder. FASEB J 2017;31:5466-77. https://doi.org/10.1096/fj.201700320R
36. Steinbacher P, Tauber M, Kogler S, Stoiber W, Resch H, Sanger AM. Effects of rotator cuff ruptures on the cellular and intracellular composition of the human supraspinatus muscle. Tissue Cell 2010;42: 37-41. https://doi.org/10.1016/j.tice.2009.07.001
37. Talarek JR, Piacentini AN, Konja AC, Wada S, Swanson JB, Nussenzweig SC, et al. The MRL/MpJ mouse strain is not protected from muscle atrophy and weakness after rotator cuff tear. J Orthop Res 2020;38:811-22. https://doi.org/10.1002/jor.24516
38. Tyanova S, Temu T, Sinitcyn P, Carlson A, Hein MY, Geiger T, et al. The Perseus computational platform for comprehensive analysis of (prote)omics data. Nat Methods 2016;13:731-40. https://doi.org/10.1038/nmeth.3901
39. Wang Z, Liu X, Davies MR, Horne D, Kim H, Feeley BT. A mouse model of delayed rotator cuff repair results in persistent muscle atrophy and fatty infiltration. Am J Sports Med 2018;46:2981-9. https://doi.org/10.1177/0363546518793403
40. Wieser K, Joshy J, Filli L, Kriechling P, Sutter R, Furnstahl P, et al. Changes of supraspinatus muscle volume and fat fraction after successful or failed arthroscopic rotator cuff repair. Am J Sports Med 2019;47:3080-8. https://doi.org/10.1177/0363546519876289
41. Wosczyna MN, Rando TA. A muscle stem cell support group: coordinated cellular responses in muscle regeneration. Dev Cell 2018;46: 135-43. https://doi.org/10.1016/j.devcel.2018.06.018
42. Yamaguchi K, Ditsios K, Middleton WD, Hildebolt CF, Galatz LM, Teefey SA. The demographic and morphological features of rotator cuff disease. A comparison of asymptomatic and symptomatic shoulders. J Bone Joint Surg Am 2006;88:1699-704. https://doi.org/10.2106/jbjs.E.00835
43. Yli-Karjanmaa M, Clausen BH, Degn M, Novrup HG, Ellman DG, Toft-Jensen P, et al. Topical administration of a soluble TNF inhibitor reduces infarct volume after focal cerebral ischemia in mice. Front Neurosci 2019;13:781. https://doi.org/10.3389/fnins.2019.00781
44. Zhang C, Wang C, Li Y, Miwa T, Liu C, Cui W, et al. Complement C3a signaling facilitates skeletal muscle regeneration by regulating monocyte function and trafficking. Nat Commun 2017;8:2078. https://doi.org/10.1038/s41467-017-01526-z
45. Zumstein MA, Ladermann A, Raniga S, Schar MO. The biology of rotator cuff healing. Orthop Traumatol Surg Res 2017;103:S1-10. https://doi.org/10.1016/j.otsr.2016.11.003